VERIFICATION AND OPTIMIZATION OF THE PHYSICS PARAMETERS OF THE ONBOARD GALILEO PASSIVE HYDROGEN MASER

Qinghua Wang, Pierre Mosset, Fabien Droz, Pascal Rochat
Temex Time
Vauseyon 29, 2000 Neuchâtel, Switzerland
E-mail: *qinghua@temextime.com*

Giovanni Busca
Kytime
Ecluse 11, 2022 Bevaix, Switzerland

Abstract

Atomic clocks represent critical equipment for a satellite navigation system. A Passive Hydrogen Maser (PHM), with its excellent frequency stability performance, has been chosen as the master clock in the Galileo navigation satellite payload, and will be the first one of its type ever to fly. Temex Neuchâtel Time is responsible for the industrialization of the Physics Package (PP) of the PHM and has been developing numbers for the PP, including Engineering Qualification, Qualification, Proto-Flight, and Flight Models in the frame of the Galileo Satellite Test Bed (GSTB-V2) and the In-Orbit Validation (IOV) phase.

This paper provides the verification results of PHM physics parameters, according to the measurement data and the theoretical analysis, for all the PPs produced up to now. A theoretical PHM physics model has been developed to extract inherent physics parameters (such as oscillation parameter, saturation factor, natural line width, various relaxation rates, and useful atomic flux) which cannot be measured directly, but are of great importance in order to evaluate the instrument performance.

I. DEVELOPMENT ACTIVITIES OF THE SPACE PASSIVE HYDROGEN MASER

Atomic clocks represent critical equipment for a satellite navigation system. The Rubidium Atomic Frequency Standard (RAFS) and Passive Hydrogen Maser (PHM) are the baseline clock technologies for the Galileo navigation payload. The adoption of a "dual technology" for the onboard clocks is dictated by the need to insure a sufficient degree of reliability (technology diversity) and to comply with the Galileo lifetime requirement of 12 years. The PHM, with its excellent frequency stability performance, has been chosen as the master clock, and will be the first one of its type ever to fly.

Temex Neuchâtel Time (TNT) is not only the supplier of the RAFS, but it is also responsible for the industrialization of the Physics Package (PP) of the PHM **[1]**. Galileo Avionica (GA), who designs the Electronics Package (EP), is responsible of the integration of the PP with the instrument (Figure 1).

Figure 1. Picture of Galileo PHM (18 kg). The Physics Package (PP) is on the top of the Electronic Package (EP).

The industrialization activity aimed at PHM design consolidation for flight production was started in January 2003, based on the Engineering Model (EM) design led by the Observatory of Neuchâtel since 2000. The main efforts for the PP in the industrialization frame have focused on the definition of repeatable and reliable manufacturing processes and assemblies, as well as the parts number and cost reductions, while keeping the critical performances unchanged (e.g. an Allan deviation of $\sigma_y(\tau) \le 1\times10^{-12}\tau^{-1/2}$ for $1s \le \tau \le 10000s$).

Two technological models (Figure 2), a Structural Model, and numbers for the PP have been developed at TNT for these objectives and to qualify the new upgraded design. In the frame of the Galileo Satellite Test Bed (GSTB-V2) and the In-Orbit Validation (IOV) phase, TNT has manufactured two Engineering Qualification Models (EQMs): a Proto-Flight Model (PFM) and a Flight Model (FM), which were delivered and tested at payload level. In addition, four Qualification Models (QM) are being manufactured and will be submitted to prolonged testing for the lifetime demonstration. The first in-orbit PHM will be validated in the Galileo experimental satellite GIOVE-B, which is now planned for launch in early 2007.

Figure 2. Technological Model with/without cover

II. MEASUREMENTS OF THE PP PARAMETERS

Before the integration with EP, the PP is tested and characterized in the thermal vacuum chamber by the Maser Test Bench, which supplies the electrical controls for the PP and monitors all operating parameters (Figures 3 and 4).

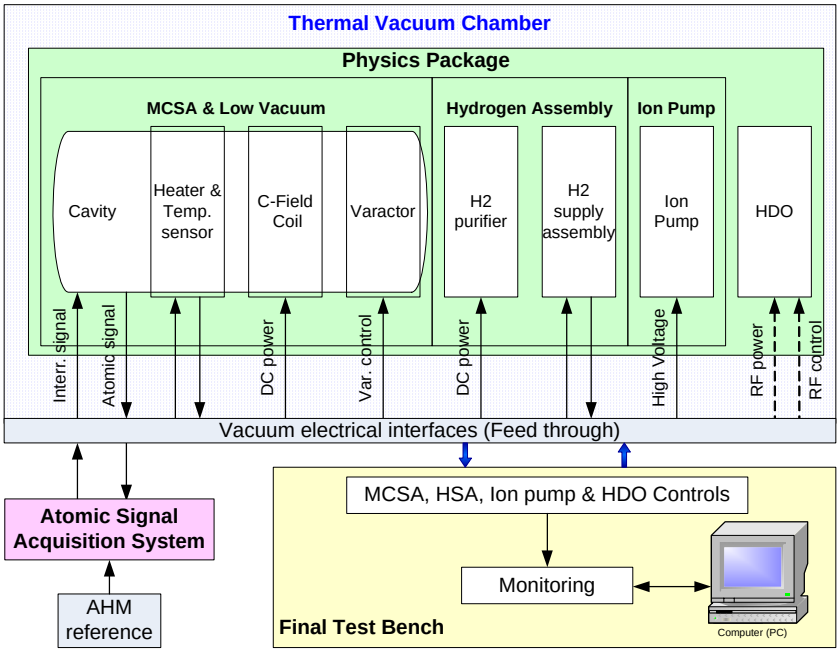

Figure 3. Test setup.

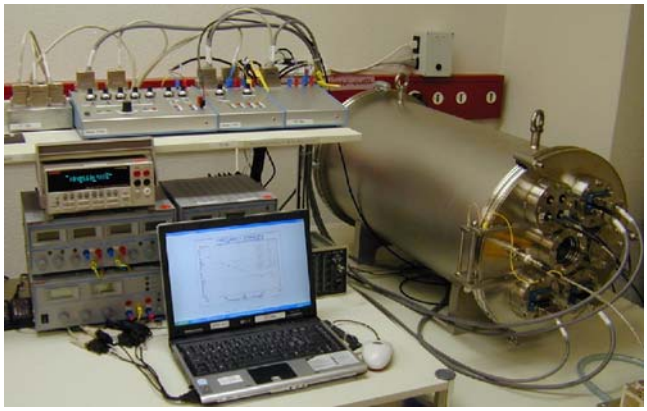

Figure 4. Maser Test Bench with Thermal Vacuum Chamber.

In order to extract the relevant physics parameters using the theoretical PHM physics model, the maser gain and the operational linewidth as the function of the interrogation power for different purifier currents have to be measured while keeping other operating parameters at nominal settings.

The maser gain and the operational linewidth are measured by the dedicated Atomic Signal Acquisition System (ASAS). The system is constituted by a RF signal processing unit controlled by two synthesized function generators in order to scan the useful frequency range step by step with the resolution of 0.001 Hz. The system gives the output level of the atomic signal vs. the interrogation frequency from which the two quantities G_0 (amplitude gain at resonance) and LW (the operational full linewidth measured at the half value of the power gain) are determined.

Figure 5 shows the atomic response of the PHM IOV-EQM PP, measured with 15 Hz span exhibiting an atomic signal gain of 3.6 dB and an operational atomic linewidth of 2.6 Hz.

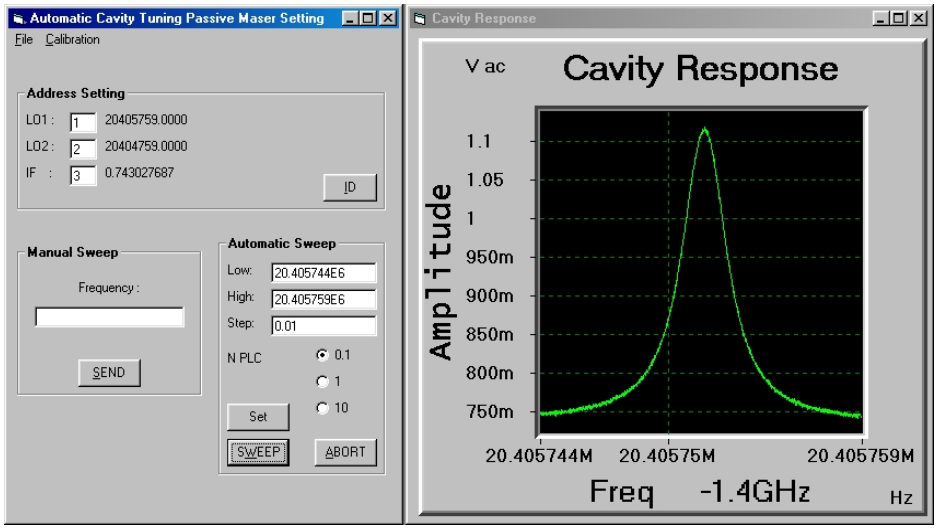

Figure 5. PHM atomic signal measured by the Atomic Signal Acquisition System for the IOV EQM.

III. EXTRACTION OF THE RELEVANT PP PARAMETERS

Based on above measurements, a theoretical PHM physics model has been developed to extract the relevant physics parameters (the oscillation parameter, the saturation factor, the natural linewidth, various relaxation rates, and the useful atomic flux) that are difficult to measure directly, but are of great importance in order to evaluate the instrument performance.

3.1 THE OSCILLATION PARAMETER AND THE SATURATION FACTOR

Unlike the self-oscillation of an active hydrogen maser, the small-sized passively operated maser is used as a microwave amplifier, having a very narrow bandwidth, by injecting in the microwave cavity an interrogation signal. The oscillation parameter α is an important parameter determining the oscillation properties of the system. The passive behavior is obtained when $\alpha < 1$.

The amplitude gain at resonance G_0 of the maser amplifier **[2]** is given by:

$$G_0 = \frac{1 + S_0}{1 + S_0 - \alpha} \tag{1}$$

where S_0 is the saturation factor at resonance, which is in proportional to the interrogation power P_{in} for a given atomic flux:

$$S_0 = k_s P_{in} \tag{2}$$

k_s is inversely proportional to $\gamma_1\gamma_2$ according to the definition of S_0, with k_c calculated as the constant independent of the atomic flux:

$$k_s = \frac{k_c}{\gamma_1\gamma_2} \tag{3}$$

From Eq. (1), the value of α is extracted from the unsaturated amplitude gain corresponding to a very low level of the interrogation signal, when $P_{in} \rightarrow 0$. The value of S_0 at larger interrogation levels is obtained from the measured (saturated) amplitude gain knowing the value of α.

Figure 6 shows the least-squares fit to the IOV-EQM PP measurement data of G_0 vs. P_{in} for three levels of H_2 flux, to find α and S_0 with k_s.

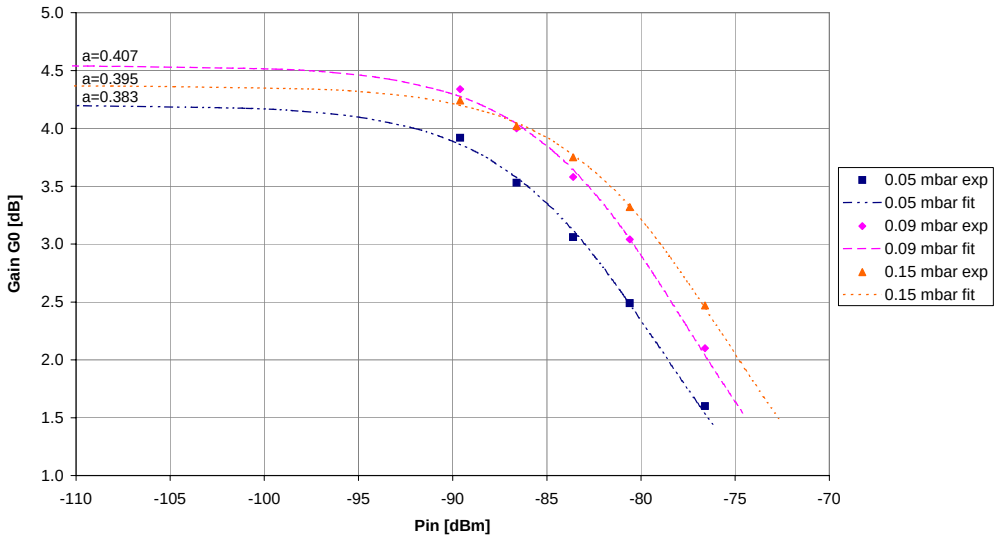

Figure 6. Atomic gain at resonance vs. interrogation power for three H_2 low pressures, and the respective oscillation parameter by a least-squares fit.

3.2 The Natural Linewidth

The transverse relaxation rate γ_2 corresponds to the natural linewidth, distinguished from the measured operational linewidth LW, which is subjected the power-broadening effect.

The amplitude gain G of the maser amplifier is **[2]**:

$$G = \left[1 + \frac{1}{1+x^2} \left(\frac{\alpha^2}{\left(1 + \frac{S_0}{1+x^2}\right)^2} - \frac{2\alpha}{1 + \frac{S_0}{1+x^2}} \right) \right]^{-\frac{1}{2}} \tag{4}$$

where x is the normalized frequency offset $x = \frac{\omega - \omega_a}{\gamma_2}$, ω is the interrogation carrier angular frequency, ω_a is the hydrogen resonance angular frequency and the cavity is assumed to be tuned to the hydrogen frequency.

The linewidth broadening factor F can be solved as the value of x at the half maximum of the power gain signal according to Eq. (4), for known α and S_0:

$$F = \sqrt{\frac{4\alpha - 4\alpha^2 + \alpha^3 - 2(\alpha-3)\alpha S_0 + 2\alpha S_0^2 - \sqrt{4(\alpha - 2 - 2S_0)^2(1 - \alpha + S_0)^2 + \alpha^2\left[(\alpha-2)^2 - 2(\alpha-3)S_0 + 2S_0^2\right]^2}}{2(\alpha - 2 - 2S_0)}} \tag{5}$$

and γ_2 can be determined from the operational linewidth:

$$\gamma_2 = \frac{\pi \times LW}{F}. \tag{6}$$

3.3 The Useful Atomic Flux and Various Relaxation Rates

These parameters can be solved from the set of equations:

$$\alpha = \frac{\mu_0 {\mu_B}^2 \eta' Q_c \psi}{\hbar V_b \gamma_1 \gamma_2} \tag{7}$$

$$\gamma_1 = \gamma_b + \frac{4}{3}\gamma_{2w} + 2k_e\psi \tag{8}$$

$$\gamma_2 = \gamma_b + \gamma_{2w} + k_e\psi \tag{9}$$

where

μ_0, μ_B and $\hbar$: constants of the magnetic permeability of vacuum, the Bohr magneton, and Planck's constant divided by 2π, respectively,

Q_c: Cavity loaded quality factor,

V_b: Storage bulb volume,

ψ: Useful H atomic flux entering the cavity in the (1,0) hyperfine state,

γ_1: Longitudinal relaxation rate, and

γ_b: Storage bulb or geometric relaxation rate; this can be calculated by

$$\gamma_b = \frac{\bar{\upsilon}\pi a^2}{4V_b\left(1+\frac{3L}{8a}\right)} \tag{10}$$

where $\bar{\upsilon}$ is the mean velocity of hydrogen atoms, and L and a are the length and radius of the exit tube of the storage bulb, respectively; this value is constant for all our PP.

γ_{2w}: Transverse wall relaxation rate, due to atomic collisions with the wall of the storage bulb.

A magnetic relaxation rate should be added theoretically to Eqs. (8-9). This term is, however, negligible for our configuration and is neglected.

The last terms of Eq. (8-9) are beam-density-dependent, contributed by the spin-exchange relaxation rate. k_e is considered to be a variable for different PPs.

In Eq. (7), the filling factor η' relates to the coupling between the atomic medium and the microwave field. It is defined by

$$\eta' = \frac{V_b}{V_c}\frac{\langle H_z\rangle_b^{\,2}}{\langle H^2\rangle_c} \tag{11}$$

where V_c is the overall volume of the cavity space, $\langle H_z\rangle_b^{\,2}$ is the square of the average amplitude of the axial component of the magnetic field within the bulb volume, and $\langle H^2\rangle_c$ is the quadratic average value of the magnetic field amplitude within the overall microwave cavity volume.

It is challenging to obtain the value of η' by the rigorous theoretical solution for such a complicated magnetron cavity structure. The numerical simulation of the electromagnetic field for the cavity-bulb assembly was performed (Figure 7) to solve for η' by integrating the H field distribution function over the bulb and the cavity volumes. The value obtained for η' is 0.40. This is the value we assume for all the PPs.

For two purifier currents A and B (corresponding to two H_2 flux setting A and B), Eqs. (7-9) give a set of six equations with known α_A, α_B, γ_{2A}, γ_{2B} and γ_b. This allows one to solve for six unknown parameters : ψ_A, ψ_B, γ_{1A}, γ_{1B}, γ_{2w} and k_e (γ_{2w} and k_e are independent of flux).

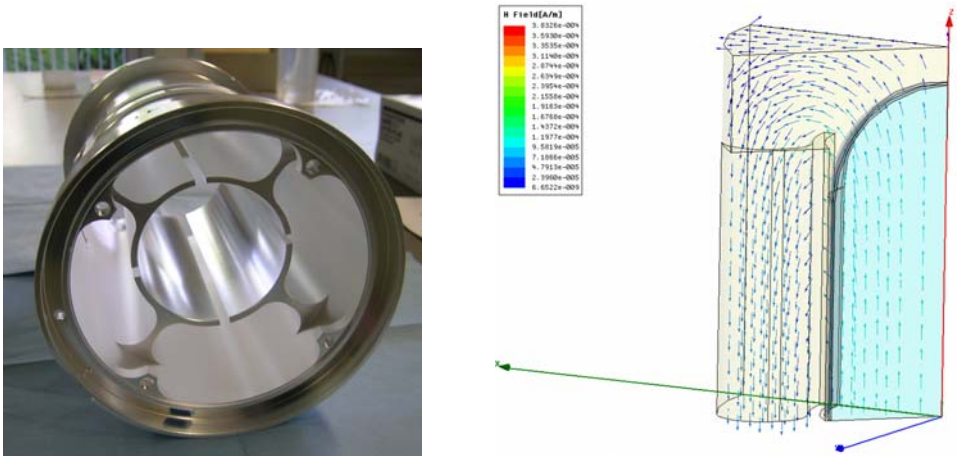

Figure 7. The TE011 magnetron microwave cavity and the magnetic field distribution simulation.

3.4 THEORETICAL FREQUENCY STABILITY AND OPTIMIZATION

We assume that the noise of the interrogation signal is negligible. In such a case, the frequency stability equation for the PHM has contributions from the thermal noise of the receiver and the PP parameters:

$$\sigma_y(\tau) = \sqrt{\frac{k_s k T F_r}{2 A_c}} \frac{(1 + S_0 - \alpha)^2}{Q_0 \alpha \sqrt{S_0}(1 + S_0)} \tau^{-\frac{1}{2}} \tag{12}$$

where k is Boltzman's constant, T is the temperature of the cavity, F_r is the noise figure of the receiver, A_c is the cavity power attenuation, and Q_0 is the atomic line quality factor:

$$Q_0 = \frac{\pi f_0}{\gamma_2}. \tag{13}$$

For a given PP, since k_s, Q_0 and α are dependent on the useful atomic flux ψ (Eqs. 3, 7-9, & 13), σ_y is now a function of ψ and S_0, i.e. respectively of the H_2 low pressure and the interrogation power.

Figure 8 shows $\sigma_y(1s)$ vs. ψ & S_0, Figure 9 shows α vs. ψ, and Figure 10 shows H_2 low pressure vs. ψ, for the IOV-EQM PP. From these figures, the optimum purifier current, the optimum interrogation power, and the maximum oscillation parameter corresponding to the best frequency stability can be obtained.

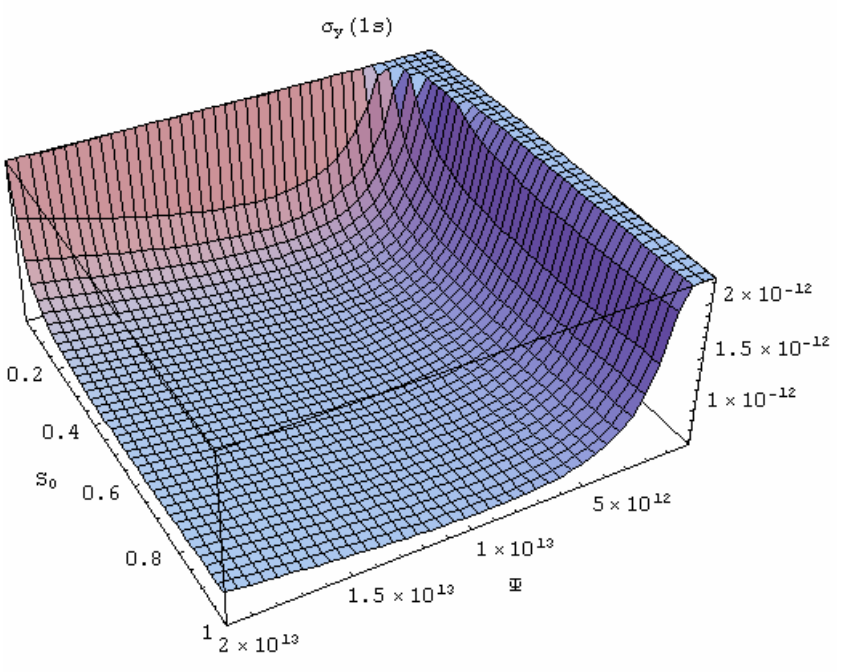

Figure 8. Theoretical Allan deviation at 1 s vs. saturation factor S_0 and useful atomic flux ψ [minimum $\sigma_y(1s)$ = 6.9·10^{-13} at S_0 = 0.37 (corresponding to interrogation power of -80 dBm) and ψ = 8.3·10^{12} atoms/s (corresponding to a low pressure of 0.10 mbar)].

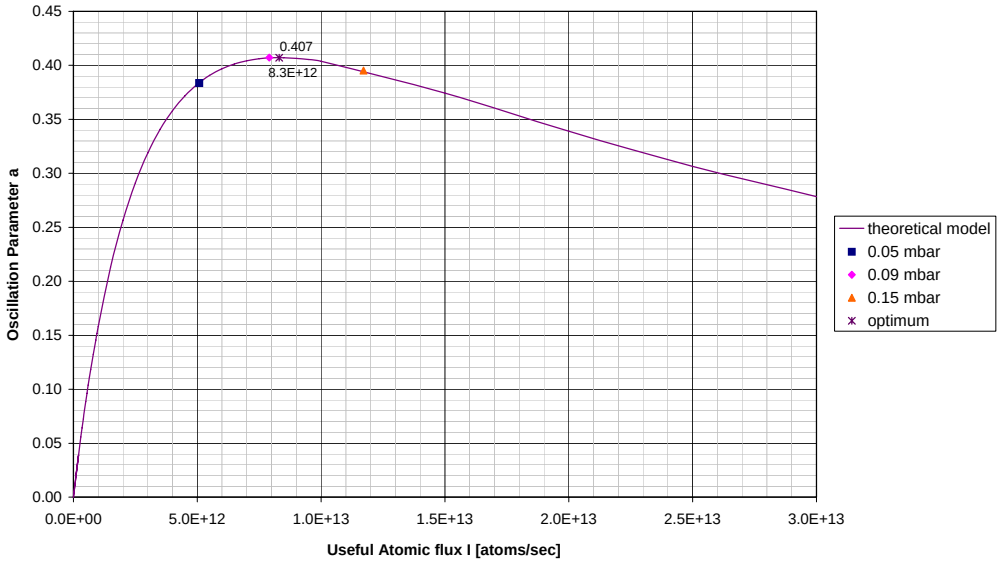

Figure 9. Calculated oscillation parameter vs. useful atomic flux for three different H_2 low pressures, and theoretical model with optimum point (α = 0.407 at ψ = 8.3·10^{12} atoms/s).

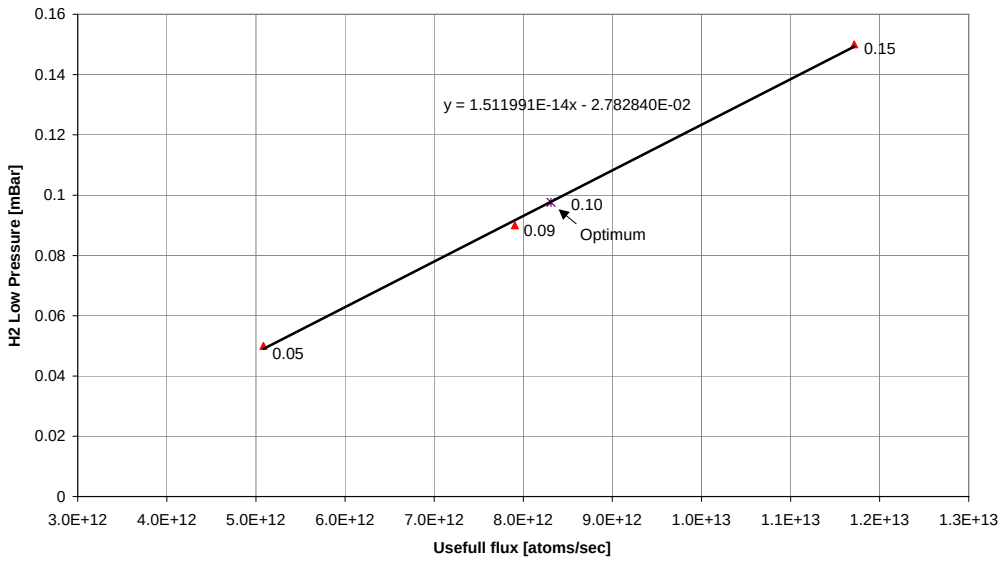

Figure 10. H_2 low pressure vs. calculated useful atomic flux and fitting for optimum value (0.10 mbar at $\psi = 8.3 \cdot 10^{12}$ atoms/s)

IV. VERIFICATION RESULTS OF PHYSICS PACKAGES

Table 1 lists the results from measurements of all PPs manufactured at TNT up to now.

In an attempt to characterize the PPs before delivering them to GA, the physics parameters were measured using the same electronics (reference electronics) with the same interrogation power.

Table 1. Comparison of PP in nominal operational condition
(blue: measurement parameters).

PP		GSTB-V2 EQM	GSTB-V2 PFM	GSTB-V2 FM1	IOV EQM	QM1
		Aug.2004	Feb.2005	Aug.2005	Jul.2006	Oct.2006
Interrogation power [dBm]		-82	-82	-82	-82	-82
H_2 low pressure [mbar]		0.1	0.1	0.08	0.09	0.09
Cavity quality factor		5800	5800	9500	9500	9500
Useful flux [atoms/s]		5.5E+12	4.1E+12	5.7E+12	7.9e+12	4.9e+12
Linewidth [Hz]	Geometric relaxation	1.2	1.2	1.2	1.2	1.2
	Wall relaxation	1.0	0.4	0.5	0.9	0.2
	Spin-exchange relaxation	0.9	0.7	0.9	1.5	1.6
	Natural (sum of above)	3.1	2.3	2.6	3.6	3.0
Atomic gain [dB]		2.1	2.5	4.8	3.4	2.8
Oscillation parameter		0.24	0.35	0.60	0.41	0.34
Theoretical Allan deviation $\sigma_y(\tau) = A\tau^{-\frac{1}{2}}$	Operational (1s)	1.4E-12	9.9E-13	3.2E-13	7.0e-13	7.3e-13
	Optimum (1s)	8.2E-13 @0.2mbar (1.1e13/s) -75dBm	8.9E-13 @0.22mbar (6.8e12/s) -81dBm	2.8E-13 @0.12mbar (6.9e12/s) -85dBm	6.9e-13 @0.1mbar (9.0e12/s) -80dBm	6.9e-13 @0.05mbar (3.2e12/s) -81dBm

The nominal operational H_2 low pressure was set to have the same H_2 consumption (< 2 bar·liter/year) for each PP. The values were selected according to the conductance calibration for each multi-hole collimator of the hydrogen dissociation bulb performed in the Technological Model before assembly of the PP. With this H_2 consumption, the useful atomic flux for 4 PP is about $5 \cdot 10^{12}$/s, varying slightly from unit to unit. The higher value of $7.9 \cdot 10^{12}$/s for the IOV EQM could come from the higher dissociation or state selection efficiency.

For the flux-independent relaxation effects, the bulb escape relaxation contributes 1.2 Hz due to the fact that we assure a constant geometry for all of the storage bulb, but the wall relaxation linewidth appears to be varying.

The average of k_e for 5 units is $6.2 \cdot 10^{-13}$, which is in good agreement with theoretical value of $5.6 \cdot 10^{-13}$, according to **[2]**.

The first two PHMs use Al cavities coated by Alodine, having a quality factor of 5800. The higher atomic gain and the oscillation parameter, leading to better frequency stability for the PFM, are due to the narrower natural linewidth, which benefits mainly from the smaller wall relaxation effect.

Since the FM1, the cavity quality factor has been increased from 5800 to 9500 by a silver coating of the magnetron cavity. A significant higher atomic gain and a higher oscillation parameter have been achieved by the quality factor improvement.

Figure 11 shows the frequency stabilities of the PPs for the GSTB-V2 EQM, PFM, and FM, measured by the reference electronics. The theoretical Allan deviations are calculated for the operational conditions corresponding to the measurements and assuming the same noise figure contributed by the receiver. The evaluation is in good agreement with the measurements of EQM and PFM, but too optimistic for FM1. In this particular case, the stability of FM1 is limited by the noise of the interrogation oscillator, which is limited to $6 \cdot 10^{-13}$ to $8 \cdot 10^{-13}$ within the maser line bandwidth. For further FM models, the local oscillator could be selected with a better short-term stability to improve the instrument short-term stability performances if there is a real need at the system level.

For a recent IOV EQM and QM1, a modification of the C-field was performed due to weight constraints. The initial assumption is that the modification could have produced a small increase of the magnetic inhomogeneity. A system is presently under study in order to estimate the associated small magnetic relaxation. The atomic gain and oscillation parameter for the IOV EQM are bigger than for the QM1. This is probably associated with a very small background vacuum obtained for the EQM. However, the estimated best frequency stabilities reach the same value for these two masers.

Figure 12 shows the preliminary measurements of PP for the IOV EQM and QM. The theoretical predications are consistent with the measurements.

As shown in the table, the best frequency stability is evaluated by optimizing the operating parameters. However, if the flux has to be increased to favor stability, which incurs a penalty to the lifetime, the trade-off for the lifetime has to be made carefully.

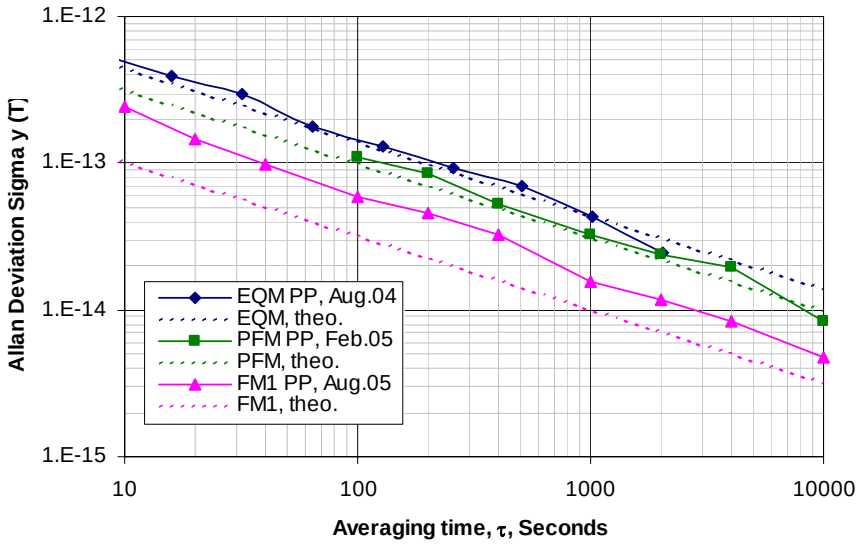

Figure 11. Measured and theoretical frequency stabilities of Physics Packages for the GSTB-V2 EQM, PFM, and FM.

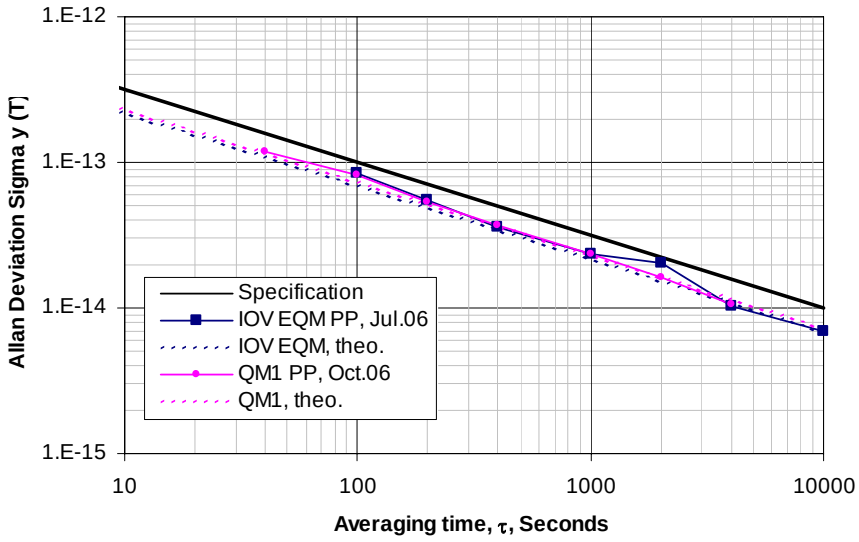

Figure 12. Measured and theoretical frequency stabilities of Physics Packages for the IOV EQM and QM1.

V. CONCLUSIONS

An efficient method for extracting the relevant maser parameters has been devised. The maser operational parameters for the five units tested are found to be within a reasonable range.

The operational flux assures the lifetime specification.

Except for the first EQM, the stability of all other units at the operational parameters settings is found to be within the specifications.

The optimum frequency stability determined by the PP parameters as demonstrated by FM1 can reach the level of $3 \cdot 10^{-13}$ at 1 s, i.e. 3 times better than the specification, but in such a case the frequency performance is limited by the local oscillator noise.

VI. REFERENCES

[1] P. Rochat, F. Droz, P. Mosset, G. Barmaverain, Q. Wang, D. Boving, U. Schmidt, T. Pike, L. Mattioni, M. Belloni, M. Gioia, and F. Emma, 2005, *"The onboard Galileo rubidium and passive maser, status and performance,"* in Proceedings of 2005 Joint IEEE International Frequency and Control Symposium and Precise Time and Time Interval (PTTI) Systems and Applications Meeting, 29-31 August 2005, Vancouver, Canada (IEEE 05CH37664C), pp. 26-32.

[2] J. Vanier and C. Audoin, 1988, **The Quantum Physics of Atomic Frequency Standards** (Adam Hilger, Bristol), Vol. **2**.

Communication information:

Qinghua Wang
Temex Time
Vauseyon 29, 2000 Neuchâtel, Switzerland
E-mail: qinghua@temextime.com
Tel: +41 32 732 96 74
Fax: +41 32 732 16 67